ETH
Eidgenössische Technische Hochschule Zürich
Swiss Federal Institute of Technology Zurich

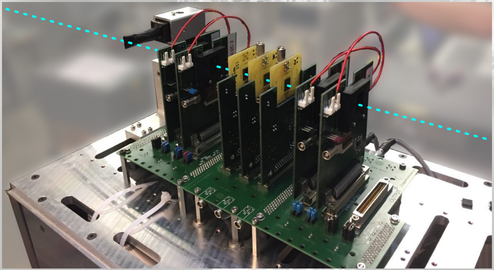

Pulse Height Analysis of 3D pCVD Diamond Detectors

RD42 Meeting - Grenoble 2019

Michael Reichmann

14th November 2019

Table of Contents

Section 1

Introduction

Diamond as Detector Material

- innermost tracking layers $\rightarrow$ highest radiation damage $\mathcal{O}\left(\mathrm{GHz/cm^2}\right)$
- $\rightarrow$ **R&D towards more radiation tolerant detector designs and/or materials**

Diamond as Detector Material

- innermost tracking layers → highest radiation damage $\mathcal{O}\left(\mathrm{GHz/cm^2}\right)$
- → **R&D towards more radiation tolerant detector designs and/or materials**

Diamond as Detector Material:

- advantageous properties
- **after $1 \cdot 10^{16}\,\mathrm{n/cm^2}$ the mean drift path in diamond larger than in silicon**

Diamond as Detector Material

- innermost tracking layers → highest radiation damage $\mathcal{O}\left(\mathrm{GHz/cm^2}\right)$
- → **R&D towards more radiation tolerant detector designs and/or materials**

Diamond as Detector Material:

- advantageous properties
- **after $1 \cdot 10^{16}\,\mathrm{n/cm^2}$ the mean drift path in diamond larger than in silicon**

Work at ETH:

- investigate signals and radiation tolerance in various detector designs:
  - Pad Detectors → whole diamond as single cell readout
  - Pixel Detectors → diamond sensor on pixel readout chip
  - 3D Pixel Detectors → 3D diamond detector on pixel readout chip

Diamond as Detector Material

- innermost tracking layers → highest radiation damage $\mathcal{O}\left(\mathrm{GHz/cm^2}\right)$
- → **R&D towards more radiation tolerant detector designs and/or materials**

Diamond as Detector Material:

- advantageous properties
- **after $1 \cdot 10^{16}\,\mathrm{n/cm^2}$ the mean drift path in diamond larger than in silicon**

Work at ETH:

- investigate signals and radiation tolerance in various detector designs:
  - Pad Detectors
  - Pixel Detectors
  - **3D Pixel Detectors** → this talk

Detectors

	II6-A2	**II6-B6**
manufacturer	II-VI Inc.	II-VI Inc.
diamond type	poly-crystal	poly-crystal
size	$\sim$4 mm $\times$ 4 mm	$\sim$4 mm $\times$ 4 mm
thickness	$\sim$500 µm	455 µm
irradiation	none	none
construction	summer 2016	summer 2017
3D drilling	Oxford	Oxford
3D cell size	150 µm $\times$ 100 µm	50 µm $\times$ 50 µm
columns	20 $\times$ 30 **(600)**	60 $\times$ 62 **(3720)**
pixel chip	PSI46digV2.1respin (CMS)	PSI46digV2.1respin (CMS)
pixel pitch	150 µm $\times$ 100 µm	150 µm $\times$ 100 µm
ganged cells	none	2 $\times$ 3 (6 cells)
bump & wire bonding	Princeton	Princeton

Table: 3D Pixel Detector Properties.

Detectors

	II6-A2	**II6-B6**
manufacturer	II-VI Inc.	II-VI Inc.
diamond type	poly-crystal	poly-crystal
size	$\sim$4 mm $\times$ 4 mm	$\sim$4 mm $\times$ 4 mm
thickness	$\sim$500 µm	455 µm
irradiation	none	none
construction	summer 2016	summer 2017
3D drilling	Oxford	Oxford
3D cell size	150 µm $\times$ 100 µm	50 µm $\times$ 50 µm
columns	20 $\times$ 30 **(600)**	60 $\times$ 62 **(3720)**
pixel chip	PSI46digV2.1respin (CMS)	PSI46digV2.1respin (CMS)
pixel pitch	150 µm $\times$ 100 µm	150 µm $\times$ 100 µm
ganged cells	none	2 $\times$ 3 (6 cells)
bump & wire bonding	Princeton	Princeton

Table: 3D Pixel Detector Properties.

- II6-A2 broke in October 2016 (chip malfunctioned) $\rightarrow$ successful re-bonding
- II6-B6 has long history of breaking ...

Measurements

	Oct 16	May 17	Aug 17	Sep 18	Oct 18	Oct 18
	PSI	PSI	PSI	CERN	CERN	PSI
II6-A2 (150 × 100)	✓	✓	✓	✓	✓	✓
II6-B6 (50 × 50)	✗	✗	✓	✗	✓	✓

Table: 3D Pixel Detector Measurements.

- at PSI: scanning particle rate, bias voltage, rise time and incident angle
- at CERN: high resolution studies at different voltages

Measurements

	Oct 16	May 17	Aug 17	Sep 18	Oct 18	Oct 18
	PSI	PSI	PSI	CERN	CERN	PSI
II6-A2 (150×100)	✓	✓	✓	✓	✓	✓
II6-B6 (50×50)	✗	✗	✓	✗	✓	✓

Table: 3D Pixel Detector Measurements.

- at PSI: scanning particle rate, bias voltage, rise time and incident angle
- at CERN: high resolution studies at different voltages

History of II6-B2:

- 06/2017 - sensor processing and detector fabrication
- 08/2017 - first measurement $\rightarrow$ high efficiency $\rightarrow$ pedestal in pulse height
- 04/2018 - several pixels malfunction $\rightarrow$ re-bump-bonding to new chip
- 06/2018 - sensor detaches while shipping $\rightarrow$ re-bump-bonding, fixate with silguard
- 10/2018 - at PSI: efficiency worsens and sensor detaches again
- 11/2019 - reprocessing and new bump bonding

Section 2

3D Pixel Detector

Working Principle

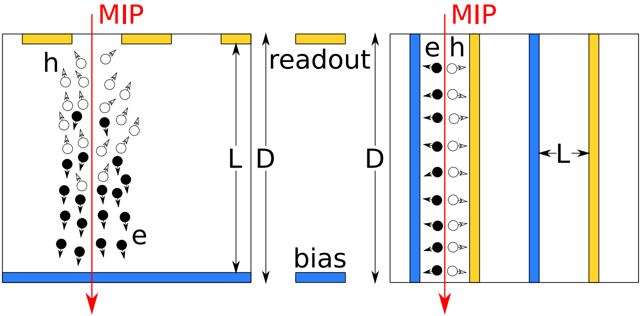

- after large radiation fluence all detectors become trap limited
- bias and readout electrode inside detector material
- same thickness $D \rightarrow$ same amount of induced charge $\rightarrow$ shorter drift distance L
- **increase collected charge in detectors with limited mean drift path (Schubweg)**

Bump Bonding

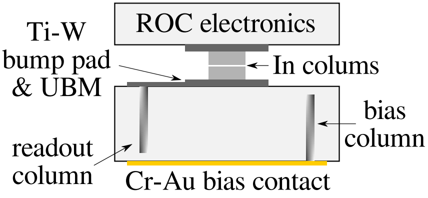

(a) Bump bond schematics

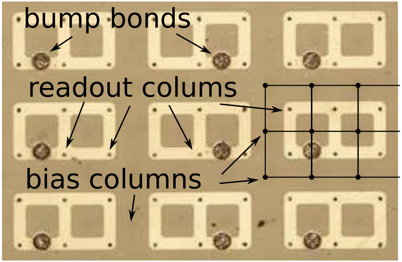

(b) 3×2 bump pads

- electrodes (columns) drilled with femto-second laser
- connection to bias and readout with surface metallisation
- ganging of cells to match pixel pitch of readout-chip (ROC)
- small gap ($\sim$15 µm) to the surface to avoid a high voltage break-through

Section 3

Reprocessing of II6-B6 in Fall 2019

Reprocessing B6

- surface cleaning and RIE (Reactive Ion Etching) at OSU
- bias metallisation at OSU
- old mask was rotated...

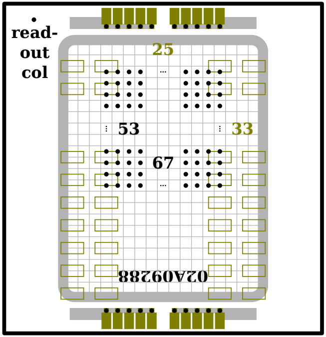

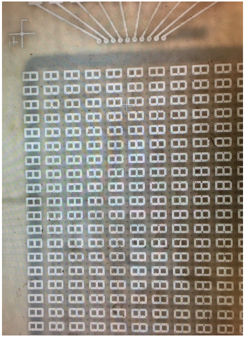

- new mask design including non drilled area for surface detector
- readout metallisation with new mask by Bert in Princeton
- bump-bonding very soon and then test at DESY

Reprocessing B6

- surface cleaning and RIE (Reactive Ion Etching) at OSU
- bias metallisation at OSU
- old mask was rotated...

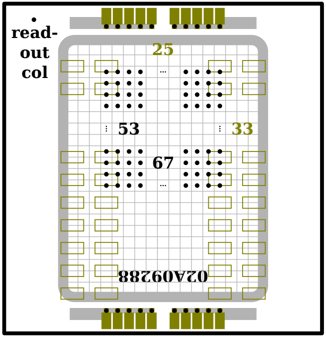

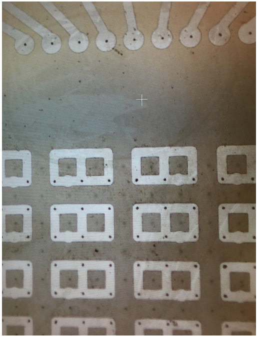

- new mask design including non drilled area for surface detector
- readout metallisation with new mask by Bert in Princeton
- bump-bonding very soon and then test at DESY

Reprocessing B6

- surface cleaning and RIE (Reactive Ion Etching) at OSU
- bias metallisation at OSU
- old mask was rotated...

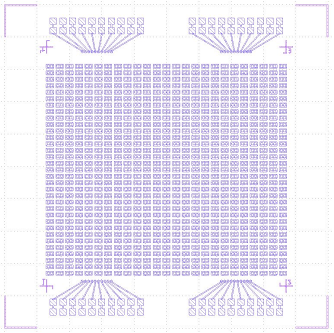

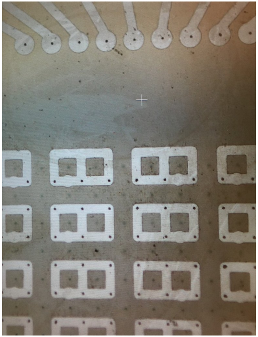

- new mask design including non drilled area for surface detector
- readout metallisation with new mask by Bert in Princeton
- bump-bonding very soon and then test at DESY

Section 4

Setup at PSI

Pixel Telescope

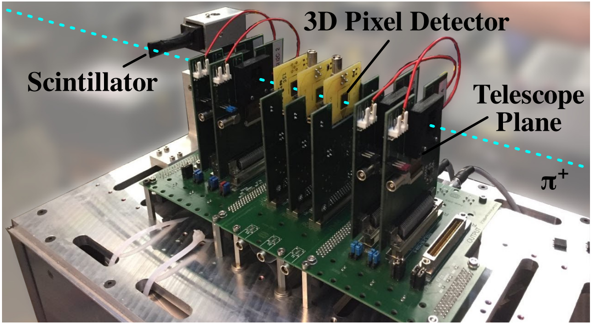

Figure: modular ETH beam telescope in pixel configuration

- 4 tracking planes → trigger (fast-OR) → adjustable area (max 8 mm × 7.8 mm)
- up to 3 DUT planes (any digital pixel detector)
- scintillator for precise trigger timing → $\mathcal{O}(1\,\mathrm{ns})$

Schematic Setup

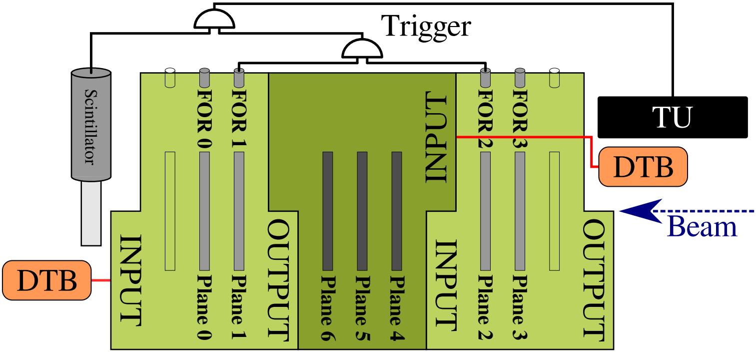

- independent telescope module for DUTs (dark green)
- scintillator → precise trigger timing of $\mathcal{O}\,(1\,\mathrm{ns})$
- Trigger Unit (TU) → strongly simplifying setup
- global trigger → (Plane 1 AND Plane 2) AND Scintillator

Section 5

Recent Results

PSI - August 2017

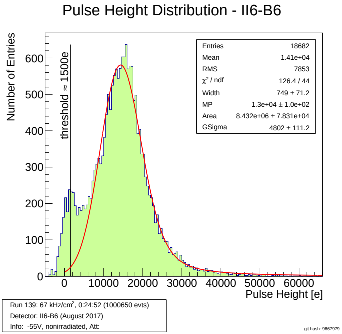

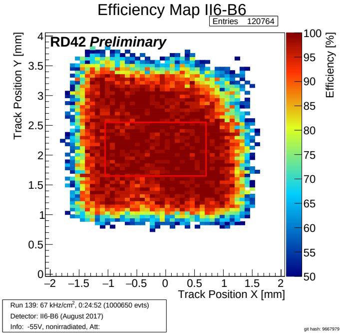

- pulse height looks OK, but "pedestal" of unknown origin (cannot be real)
  - cannot be remeasured, since the ROC was exchanged
- Langau MPV: 13 500 e
- uniform efficiency

PSI - August 2017

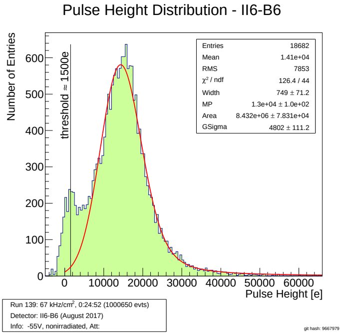

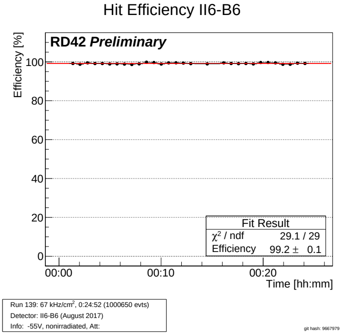

- pulse height looks OK, but "pedestal" of unknown origin (cannot be real)
  - cannot be remeasured, since the ROC was exchanged
- Langau MPV: 13 500 e
- uniform efficiency
- high efficiency of $(99.2 \pm 0.1)\,\%$

Section 6

Pulse Height Calibration

Pixel Unit Cell

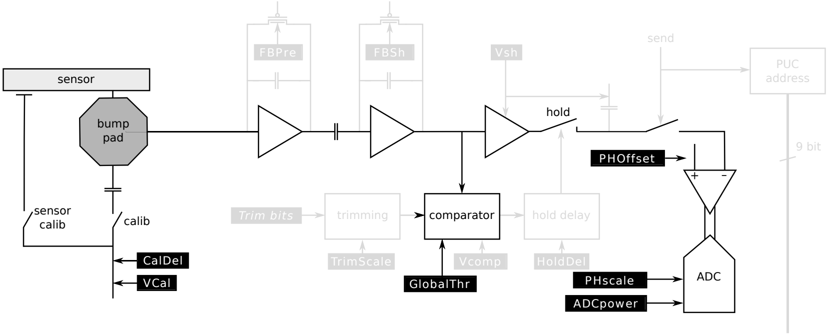

- inject calibration signal (∼ vcal) through sensor into same circuit as real signals
- shaping, amplification, threshold check
- set amplification offset
- convert to 8 bit adc value with adjustable scale → readout

ADC Calibration

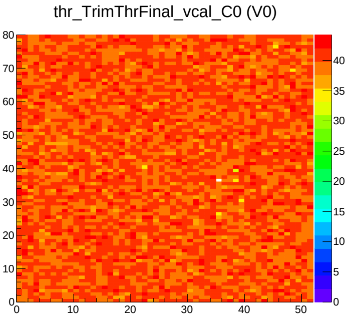

(a) Threshold Map.

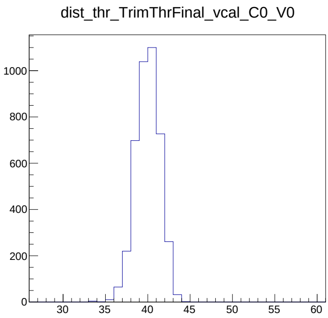

(b) Threshold Distribution.

- trim all pixels to the same threshold

ADC Calibration

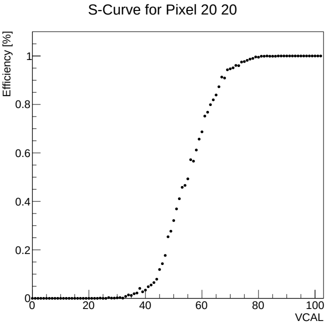

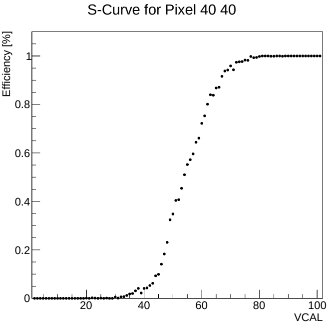

- trim all pixels to the same threshold
- means pixel start to become efficient at the tuned threshold

ADC Calibration

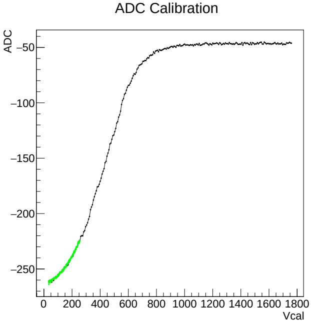

Figure: ADC calibration for single pixel.

- measure adc values for calibration pulses with different vcal
- adc follows error function and saturates for high vcal

ADC Calibration

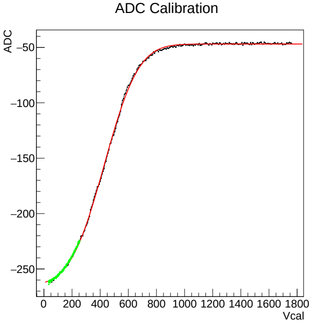

Figure: ADC calibration for single pixel with error function fit.

- measure adc values for calibration pulses with different vcal
- adc follows error function and saturates for high vcal
- fit every pixel and save fit parameters
- adjust adc offset and range with DACs of the chip

ADC Calibration - Temperature Dependence

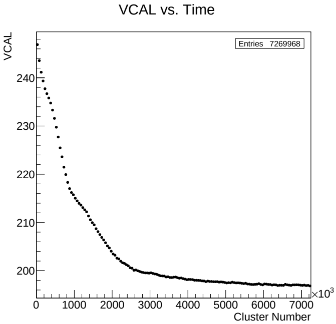

Figure: Read back VCAL inducing test-pulses with VCAL 200.

- readout chip heats up quite significantly while being in use
- adc calibration strongly temperature dependent
- inducing test pulses with VCAL 200 at room temperature
  - converting the measured ADC back to VCAL using the calibration
  - VCAL only approaches the correct value after the chip reaches the correct temperature
- $\rightarrow$ always perform calibration after heating up the chip!

ADC Calibration - Test Pulses

- chip was trimmed to 40 vcal

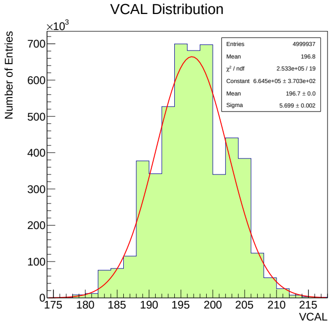

(a) 200 VCAL test pulse

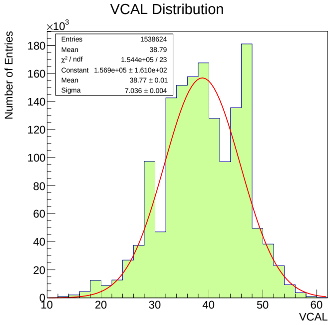

(b) 40 VCAL test pulse

- in temperature equilibrium the read back of the VCAL works well
- large sigma of the distribution allows pulse heights below threshold
- sigma gets larger for low pulse height due to bigger uncertainty in the fit

Vcal Calibration (Silicon)

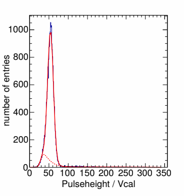

(a) Zn target.

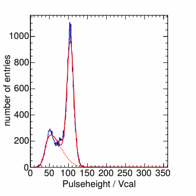

(b) Mo target.

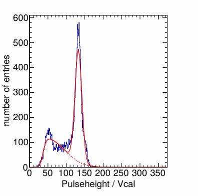

(a) Ag target.

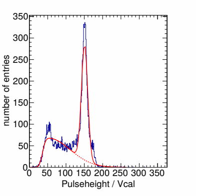

(b) Sn target.

- measure energy spectra of K_α lines of four metal targets using ADC-calibration

Vcal Calibration (Silicon)

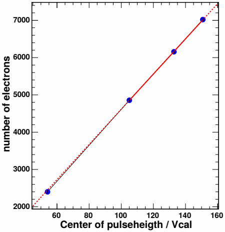

Figure: Vcal Calibration.

- measure energy spectra of K_α lines of four metal targets using ADC-calibration
- linear dependence of energy [e] and vcal
- fit K_α points with straight line (similar for each chip)
- impossible to do calibration with diamond (energy too low)

Vcal Calibration (Silicon)

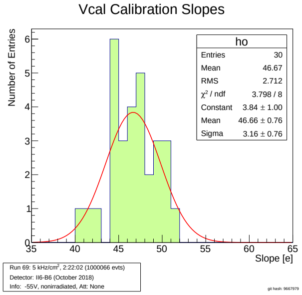

(a) Vcal slopes.

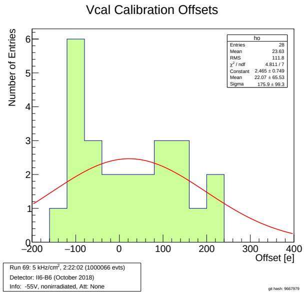

(b) Vcal offsets.

- measure energy spectra of K_α lines of four metal targets using ADC-calibration
- linear dependence of energy [e] and vcal
- fit K_α points with straight line (similar for each chip)
- impossible to do calibration with diamond (energy too low)
  - use general values from silicon: $\mathrm{e} = 46.5 \cdot vcal$

Section 7

Results

Silicon - Single Plane with Sr90

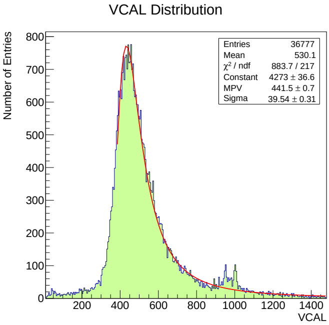

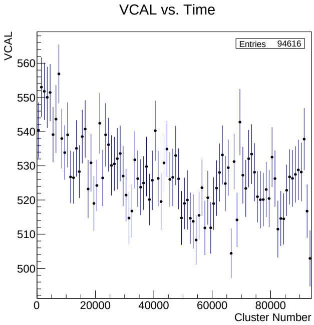

- bias voltage: $-150\,\mathrm{V}$
- thickness of silicon sensor: $285\,\mu\mathrm{m}$
- expected mean pulse height: $285\,\mu\mathrm{m} \cdot 89\,\mathrm{e}/\mu\mathrm{m} = 25\,365\,\mathrm{e}$
- measured mean pulse height: $530\,\mathrm{vcal} \cdot 46.5\,\mathrm{e}/\mathrm{vcal} = 24\,645\,\mathrm{e}$
- signal relatively stable with time

Planar CVD Diamond - Single Plane with Sr90

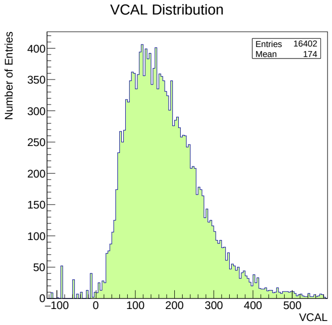

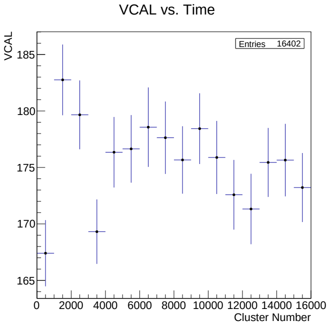

- bias voltage: $-400\,\mathrm{V}$
- thickness of diamond sensor: $\sim 500\,\mu\mathrm{m}$
- expected mean pulse height: $500\,\mu\mathrm{m} \cdot 37\,\mathrm{e}/\mu\mathrm{m} = 18\,500\,\mathrm{e}$
- measured mean pulse height: $174\,\mathrm{vcal} \cdot 46.5\,\mathrm{e}/\mathrm{vcal} = 8100\,\mathrm{e}$
- signal stable with time

Section 8

Conclusion

Conclusion

- many different measurement of both 3D diamond detectors
  - start analyse more data!
- X-ray pulse height calibration can hardly be performed on diamond
  - need to use estimate from silicon
- adc calibration is very temperature dependent
  - need to perform calibration after chip heated up
- pulse height can significantly fluctuate below threshold
- pulse height results on single planes very reasonable without distributions below threshold

Del Fin

Section 9

Backup

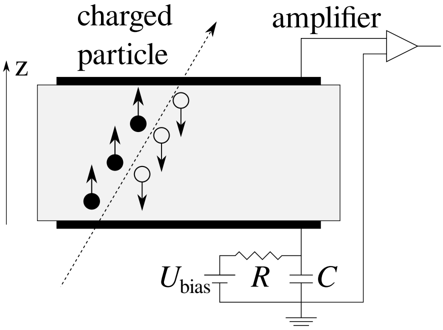

(a) Detector Schematics

(b) 15 cm ⌀ pCVD Diamond Wafer

- detectors operated as ionisation chambers
- metallisation on both sides
- poly-crystals produced in large wafers